

Received: 02.11.2024

Accepted: 27.11.2024

Research Article

Evaluation of Phytochemical Interactions of *Syzygium cumini* Bark with Xanthine Oxidase, HGPRT, and Adenosine Deaminase: Target Identification, Active Site Prediction, ADMET Analysis and Molecular Docking for Hyperuricemia Management

Kanaka Raju Addipalli, Aruna Kumari Dokkada, Gana Manjusha K¹

Vignan Institute of Pharmaceutical Technology, Besides VSEZ, Kapujaggaraju peta, Visakhapatnam-530049, Andhra Pradesh, India

Abstract: *Syzygium cumini* (Jamun) is recognized for its rich bioactive profile and potential therapeutic applications, particularly for conditions like hyperuricemia and oxidative stress. This study employs a comprehensive approach to identify and evaluate the pharmacokinetic properties, ADMET (Absorption, Distribution, Metabolism, Excretion, and Toxicity) characteristics, and toxicological profiles of 13 phytochemicals from *S. cumini* bark. Target prediction linked several of these compounds to hyperuricemia-related enzyme inhibition. ADMET analysis, along with Lipinski's rule of five, confirmed their drug-likeness and bioavailability, identifying candidates such as 11-O-galloylbergenin, Betulinic acid, and Gallic acid as promising due to their ability to permeate biological barriers and interact with P-glycoprotein. Molecular docking highlighted notable binding affinities for three key enzymes involved in hyperuricemia: Xanthine oxidase (3NRZ), Hypoxanthine-Guanine Phosphoribosyltransferase (HGPRT) (3GGC), and Adenosine deaminase(1O5R). Specifically, 11-O-galloylbergenin, Ellagitannin, and Canthaxanthin exhibited strong interactions, with binding energies of -10.8 kcal/mol, -9.7 kcal/mol, and -11.1 kcal/mol, respectively. These results suggest their potential as enzyme inhibitors, supporting their development as natural treatments for uric acid-related conditions. Toxicity assessments confirmed that most compounds possess safe profiles, underscoring *S. cumini*'s value in producing safe, plant-based therapeutics. This work provides a foundation for future research on *S. cumini*'s bioactive compounds, encouraging further in vivo studies to validate their efficacy and safety for clinical applications.

Keywords: Active site Prediction, ADMET analysis, Docking, Hyperuricemia, *Syzygium cumini*

1. Introduction

Hyperuricemia is a metabolic condition characterized by increased serum uric acid (SUA) levels in extracellular fluids and tissues, along with a decrease in uric acid excretion [1]. It is clinically defined by SUA concentrations of ≥ 7.0 mg/dL (416.0 $\mu\text{mol/L}$) in men and ≥ 6.0 mg/dL (357.0 $\mu\text{mol/L}$) in women [2]. This condition is linked to several risk factors, including a diet rich in purines, alcohol intake, certain medications, hypertension, hypothyroidism, and obesity. Furthermore, factors like higher socioeconomic status, smoking history, and alcohol consumption also elevate the likelihood of developing hyperuricemia [3, 4].

1.1. Prevalence of Hyperuricemia

Hyperuricemia is a common condition worldwide, especially in middle- and high-income nations. Its prevalence differs widely, influenced by factors like geographic region, ethnicity, local dietary patterns, and economic status. Recent data show a rising trend in hyperuricemia cases globally, with prevalence rates reported to range between 2.6% and 36% across various populations [2, 3]. Table 1 Summarises hyperuricemia prevalence by country, with data separated by gender where available [2]. Uric acid (UA), a heterocyclic organic compound with the molecular formula $\text{C}_5\text{H}_4\text{N}_4\text{O}_3$ (7,9-dihydro-1H-purine-2,6,8(3H)-trione), has a molecular weight of 168 Da. First identified by the

¹ Corresponding Authors

e-mail: manjusha.kondepudi.g@gmail.com

Kanaka Raju Addipalli, Aruna Kumari Dokkada, Gana Manjusha K

Swedish chemist Carl Wilhelm Scheele, UA plays a central role in the purine metabolism, both exogenous and endogenous [5]. It serves as a critical intermediate, without which the synthesis of nucleic acids such as deoxyribonucleic acid (DNA) would not occur, making it indispensable to life.

The dietary intake, particularly of animal proteins, significantly contributes to the exogenous pool of purines. Endogenously, the liver, intestines, muscles, kidneys, and vascular endothelium are the major sites of UA production [6].

Table 1. Hyperuricemia Prevalence in different countries

Country	Overall Prevalence (%)	Male Prevalence (%)	Female Prevalence (%)
United States (NHANES)	21.0	-	-
Australia	16.6	-	-
Finland	48.0	60.0	31.0
New Zealand	17.0	27.8	8.8
Ireland	24.5	25.0	24.1
Croatia	9.9	-	-
Russia	16.8	-	-
Turkey	12.1	19.0	5.8
Qatar	21.2	-	-
South Korea (KNHANES)	11.4	17.0	5.9
Mexico	20.6	-	-
Niger	17.2	25.0	13.7
French Polynesia	71.6	-	-
India	44.6	-	-
Jordan	28.1	-	-
Sub-Saharan Africa	31.8	-	-
Thailand	10.6	18.4	7.8
Saudi Arabia	8.4	-	-
Bangladesh	9.3	-	-

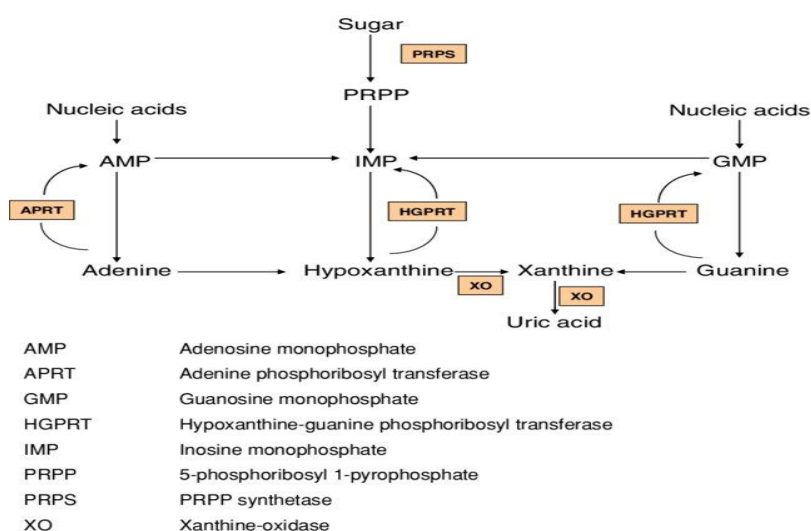


Figure 1. Metabolism of Uric acid ; Copyright CC 2009 @ Justine Bacchetta

The metabolism of UA involves a complex sequence of enzymatic reactions that convert purine nucleotides, adenine and guanine, into UA (Figure

1). Adenosine monophosphate (AMP) undergoes deamination or dephosphorylation to form inosine, while guanine monophosphate (GMP) is

transformed into guanosine [5]. These nucleosides are then further processed by purine nucleoside phosphorylase (PNP) to yield hypoxanthine and guanine, respectively. Hypoxanthine is oxidized to xanthine by xanthine oxidase (XO), while guanine is deaminated to xanthine by guanine deaminase. Subsequently, xanthine is converted to UA, which accumulates in higher primates [7]. In contrast, most mammals further break down UA into allantoin, a more water-soluble metabolite, through the action of the enzyme uricase, which humans lack [8,9].

The normal reference interval of uric acid in human blood is 1.5 to 6.0 mg/dL in women and 2.5 to 7.0 mg/dL in men. Hyperuricemia has been defined as ≥ 7.0 mg/dL in men, and ≥ 5.7 or ≥ 6 mg/dL in women. Hypouricemia is defined as a serum UA of ≤ 2.0 mg/dL [2].

In humans, the kidneys and gastrointestinal tract work together to eliminate uric acid (UA), with the kidneys handling about two-thirds of the load. UA undergoes filtration in the glomeruli, followed by reabsorption (about 90%) in the S1 segment and secretion mainly in the S2 segment of the proximal tubule, balancing reabsorption and excretion. Disruptions in this balance can lead to hyperuricemia, associated with gout, kidney dysfunction, and cardiovascular issues [10-13].

Hyperuricemia results from an imbalance in UA production and excretion, often due to malfunctions in key urate transporters like URAT1, GLUT9, and ABCG2 [14-16]. These transporters help control serum uric acid levels, with ABCG2 mutations notably contributing to hyperuricemia by reducing urate secretion. URAT1, encoded by SLC22A12, acts as the main apical urate transporter in the kidney, while GLUT9 (SLC2A9) specializes in urate rather than glucose transport [7]. Variants of GLUT9 are implicated in gout and cardiovascular diseases. GLUT9 isoforms are distributed differently in the body, with GLUT9a being widespread and GLUT9b primarily in the liver and kidneys [9].

Additionally, excess UA production can result from high-purine or fructose-rich diets, genetic mutations, and environmental factors. For example, fructose rapidly depletes ATP, raising UA levels, and genetic deficiencies, such as in hypoxanthine-guanine phosphoribosyltransferase (HGPRT), can further increase blood uric acid.

1.2. Xanthine Oxidase (XO)

Xanthine oxidoreductase (XOR) is a critical enzyme in purine catabolism, facilitating the oxidation of hypoxanthine to xanthine and xanthine to uric acid. XOR can function in two forms: xanthine dehydrogenase (XDH), which uses NAD⁺ as an electron acceptor, and xanthine oxidase (XO), which uses oxygen. XO produces reactive oxygen species (ROS), including hydrogen peroxide (H₂O₂) and superoxide anion (O^{•-}), which can be cytotoxic in certain conditions. XDH also generates ROS when NAD⁺ is scarce. XOR is a metallo flavoprotein, containing subunits with redox centres made up of molybdenum, flavin adenine dinucleotide (FAD), and iron-sulphur clusters. Each purine oxidation reaction occurs at the molybdenum center, with electron transfer occurring through the iron-sulphur clusters. XOR activity is regulated at multiple levels, including transcriptional control by nutritional factors, hormones, and vitamins [17-23].

XOR is highly expressed in organs like the liver, intestines, and blood, but its activity is limited in tissues such as the brain and heart. Inhibitors like allopurinol are used to treat diseases related to elevated uric acid, such as gout and heart failure. However, XOR also has antimicrobial properties, producing ROS that inhibit bacterial growth. Under certain conditions, XOR contributes to the production of nitric oxide (NO), which combines with ROS to form peroxynitrite (ONOO⁻), a potent oxidant involved in cardiovascular diseases and oxidative damage. Elevated XOR activity has been linked to conditions such as hypertension, dyslipidemia, diabetes, and atherosclerosis [24-28].

1.3. Adenosine Deaminase (ADA)

Adenosine deaminase (ADA) is an enzyme that breaks down purines, converting adenosine and deoxyadenosine into inosine and deoxyinosine. This enzyme is found throughout the body in both tissues and fluids. Humans have three different isoforms of ADA: ADA-1, ADA-2, and ADA-3 [29]. ADA-1 exists in two forms: a low-molecular-weight form and a complex bound to the protein CD26. Although the mechanisms of ADA-1 and ADA-2 are similar, ADA-2, found only in multicellular organisms, has a growth factor function (ADGF) and is primarily located in

Kanaka Raju Addipalli, Aruna Kumari Dokkada, Gana Manjusha K

extracellular spaces. Structurally, ADA adopts a TIM barrel fold with eight surrounding helices and additional helices that modify its regular structure [30]. The enzyme's active site is located at the C-terminal side of the barrel, containing a zinc ion crucial for catalysis. Zinc stabilizes the enzyme and is required for the water molecule transfer during the enzymatic reaction [31]. ADA-1 also plays a role in modulating extracellular adenosine levels as an ectoenzyme. In cells, ADA interacts with the transmembrane protein CD26, promoting immune responses through T-cell co-stimulation [32].

1.4. Hypoxanthine-Guanine Phosphoribosyl Transferase (HGPRT)

The enzyme HGPRT plays a pivotal role in purine salvage, essential for cellular functions. In the absence of HGPRT, hypoxanthine and guanine cannot be recycled and are instead degraded into uric acid, which, due to its limited solubility, can accumulate in the body [33]. Elevated uric acid levels can lead to crystallization in joints, causing gouty arthritis, or form solid masses known as tophi in subcutaneous tissues. Additionally, it can lead to kidney stone formation, as uric acid is primarily excreted through the kidneys. The clinical manifestations of this condition arise from the poor solubility of uric acid in the body. HGPRT facilitates the recycling of purine bases by catalyzing the conversion of hypoxanthine and guanine to IMP and GMP using 5-phosphoribosyl-alpha-pyrophosphate (PRPP) as a co-substrate. A deficiency in HGPRT leads to Lesch-Nyhan syndrome, a rare X-linked disorder characterized by the accumulation of purines and PRPP. The excess PRPP increases purine synthesis de novo, leading to overproduction of uric acid. Lesch-Nyhan syndrome results in severe gout, kidney problems, intellectual disability, neurological issues, and self-harming behaviors due to the buildup of uric acid from infancy [34].

1.5. Hyperuricemia And Kidney Disease

Kidney damage from elevated uric acid (UA) levels, or hyperuricemia, is traditionally linked to UA crystal deposits that can obstruct tubules and induce inflammation, leading to reduced glomerular filtration rates (eGFR) [35]. Excessive UA excretion (hyperuricosuria: >800 mg/day in men, >750 mg/day in women) causes acute kidney

injury by depositing crystals in the collecting ducts, triggering tubulointerstitial damage and further lowering eGFR [36-40].

Beyond crystal effects, hyperuricemia promotes renal vasoconstriction via endothelial dysfunction, renin-angiotensin system activation, and epithelial-to-mesenchymal changes in renal cells [36-40]. Intracellularly, UA acts as a pro-oxidant, stimulating NADPH oxidase and impairing endothelial function by increasing oxidative stress and reducing nitric oxide bioavailability [41-42]. Lowering UA with allopurinol has shown potential in improving endothelial function [43,44].

In animal studies, hyperuricemia elevates cyclooxygenase-2 expression and promotes vascular smooth muscle cell proliferation in preglomerular arterioles, contributing to hypertension and kidney damage [36]. Rats with hyperuricemia experience increased renin-angiotensin activity, glomerular hypertension, and preglomerular vasculopathy, which disrupts arteriolar autoregulation and reduces renal blood flow and eGFR [36-37, 46-47]. UA also drives tubulointerstitial fibrosis through epithelial-to-mesenchymal transitions in renal cells [48].

1.6. *Syzygium cumini*

Syzygium cumini (L.) Skeels, also known by its synonyms *Eugenia jambolana* Lam., *Syzygium jambolana* Dc., or *Eugenia cumini* Druce, is commonly referred to as Jamun, Jambul, or black plum. It belongs to the Myrtaceae family and is cultivated in various regions, including Pakistan, India, Indonesia, Afghanistan, and Myanmar [49]. In ancient medicinal systems such as Siddha, Tibetan, Unani, Sri Lankan, and Ayurveda, *S. cumini* has been widely used to address ailments such as diarrhoea, menstrual irregularities, obesity, haemorrhages, and vaginal discharge. Traditionally, a hot water extract made from dried fruits is employed to alleviate stomach inflammation [50]. For urinary tract inflammation, it is customary to drink one glass of *S. cumini* fruit juice mixed with half a teaspoon of stem bark powder daily. Additionally, a mixture of *S. cumini* leaves and cinnamon is thought to be effective in treating childhood diarrhoea. Storing the juice of ripe fruits for three days before oral administration is a traditional remedy for gastric issues.

Syzygium cumini leaves are also utilized for treating kidney problems, indigestion, and hyperglycemia, while the seeds are recognized for their role in managing hyperglycemia. The bark of *S. cumini* has been used to treat intestinal inflammation, hyperglycemia, and headaches. Moreover, bark juice is traditionally used as an anti-inflammatory agent, and it has been administered to women with recurrent miscarriages. Various anatomical parts of the plant, such as the seed, pulp, skin, bark, and leaves, have been documented for their antioxidant activity, anti-inflammatory properties, cytotoxic potential, and hypoglycemic effects. Additionally, studies highlight *S. cumini*'s chemopreventive, cardioprotective, antipyretic, hepatoprotective, chemopreventive, and antinociceptive properties [51-54].

This study aims to explore the therapeutic potential of *Syzygium cumini* bark in addressing hyperuricemia and its related complications. The research includes a detailed investigation of the bioactive compounds present in *S. cumini*, predictions of potential molecular targets, evaluation of bioactivity, assessment of toxicity, pharmacokinetic properties, and *in silico* docking studies.

2. Computational Method

2.1. Screening of Phytochemicals

To gather comprehensive information on the Phytochemicals of *S. cumini*, an extensive literature review was conducted across various databases such as Google Scholar, PubMed, and CNKI, using both the botanical name *S. cumini* and related terms [55].

2.2. Target Prediction

Swiss Target Prediction (<http://www.swisstargetprediction.ch/>), accessed on 4th October 2024) was utilized to forecast drug targets based on the structural similarity (2D and 3D) of known compounds [56]. The SMILES formats of the active ingredients of *S. cumini* were retrieved from the PubChem database, uploaded into the Swiss Target Prediction platform, and analyzed with "Homo sapiens" as the specified species. A screening threshold of "Probability > 0.01" was applied to predict potential targets for the active compounds. Hyperuricemia-related targets were sourced from the GeneCards database

(<https://www.genecards.org/>, accessed on October 6th, 2024). By inputting the term "Hyperuricemia" into the search tool of the database, relevant targets were identified. Using the Venny 2.1.0 platform (<https://bioinfogp.cnb.csic.es/tools/venny/>, accessed on October 6th, 2024), the intersection between hyperuricemia-associated targets and the predicted targets of *Syzygium cumini* bark was analyzed to pinpoint potential targets for its anti-hyperuricemic effects.

2.3. ADMET analysis

The phytochemicals were assessed using the Swiss ADME database (<http://www.swissadme.ch/>), accessed on 5th October 2024) [57]. Two main ADME indices were considered: GI absorption, which evaluates the drug's absorption potential in the gastrointestinal tract after oral administration, and drug-likeness, which determines the molecule's potential to become an orally bioavailable drug.

2.3.1. Compound Toxicity Assessment

To assess the potential adverse and toxic effects of the selected phytochemicals, https://tox.charite.de/protox3/index.php?site=compound_search_similarity Accessed in 5th October 2024 was employed [58].

2.4. Molecular Docking

2.4.1 Protein preparation

The Protein structures related to uric acid regulation are Xanthine oxidase (PDB ID: 3NRZ), HGPRT (PDB ID:3GGC) and Adenosine deaminase (PDB ID: 1O5R) downloaded from the RCSB Protein Data Bank (<https://www.rcsb.org/structure>) in PDB format. Further, the downloaded protein structures were cleaned and prepared by removing water molecules and previously bound ligand groups. The binding pocket analysis and all the protein preparation tasks were done using CASTp server (Computed Atlas of Surface Topology of protein). Further the protein structure was protonated by the addition of polar hydrogen atoms [59, 60].

2.4.2 Active site prediction

The three selected proteins retrieved from RCSB Protein Data Bank were analyzed for binding pocket compatibility using the active site prediction server CASTp (Computed Atlas of Surface Topology of Protein). The CASTp server identifies multiple binding pockets, each with distinct surface

area, volume dimensions, and residue counts. In this study, we selected binding pockets with the largest surface areas and volumes for docking analysis [60].

2.4.3 Ligand preparation

The structures of thirteen phytochemicals found in *Syzygium cumini*, including 2-butenic acid (PubChem CID: 637090), 11-o-galloylbergenin (PubChem CID: 56680102), bergenin (PubChem CID: 66065), betulinic acid (PubChem CID: 64971), ellagic acid (PubChem CID: 5281855), ellagitannin (PubChem CID: 10033935), epi-friedelanol (PubChem CID: 119242), eugenin (PubChem CID: 10189), friedelin (PubChem CID: 91472), gallic acid (PubChem CID: 370), myricetin (PubChem CID: 5281672), canthaxanthin (PubChem CID: 5281227) and kaempferol (PubChem CID: 5280863) were retrieved from the PubChem database (<https://pubchem.ncbi.nlm.nih.gov/>). These ligands were downloaded in 2D SDF format using the PyRx tool to identify the best hits for the target proteins. Docking study was conducted using Auto Dock Vina package of PyRx 0.8 from MGLTools (<https://ccsb.scripps.edu/mgltools/>), following default settings [61].

2.4.4 Molecular docking studies

Molecular docking was performed for thirteen ligands with these three proteins using Auto Dock Vina package of PyRx 0.8 (available at <https://pyrx.sourceforge.io/>). The PDB file format of the target proteins was loaded in PyRx 0.8 and then converted as a macromolecule in the PDBQT file format. The structure of ligands was subjected to energy minimization (EM) and converted to the PDBQT format using the Open Babel plugin of PyRx [62,63]. The ligand structures and targeted protein were selected in AutoDock Vina, and a grid box was selected to cover the residues of the binding site with dimensions retrieved from CASTp X: 89.22 Å, Y: 70.15 Å, and Z: 73.41 Å, with center X: 13.458, Y: -17.757, and Z: .37.318 (xanthine oxidase), X: 70.95 Å, Y: 71.93 Å, and 89.52 Å, with center X: 9.002, Y: 55.15, and Z: 14.78 (HGPRT) and X: 89.22 Å, Y: 70.15 Å, and Z: 73.41 Å, with center X: 13.458, Y: -17.757, and Z: .37.318 (Adenosine deaminase) using the Vina workspace. The exhaustiveness was set to default at 8. Further, the best pose with highest negative binding affinity and

zero RMSD was selected for each ligand. Additionally, the interaction between docked protein and ligand was visualized, and saved conformations were analyzed with the help of BIOVIA Discovery Studio [64].

3. Results and discussion

3.1. Screening of Phytochemicals

Google scholar, China National Knowledge Infrastructure (CNKI), and PubMed databases were used to search for the active ingredients of *Syzygium cumini*. After collecting and removing the repeated values a total of 13 phytochemicals were obtained [52-54, 65] (Table 2).

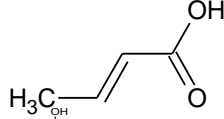
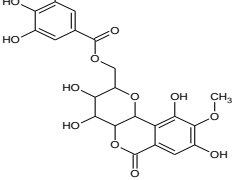
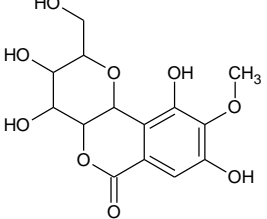
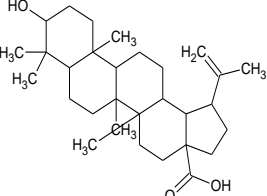
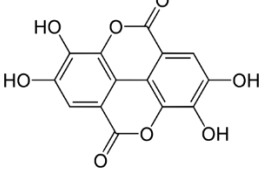
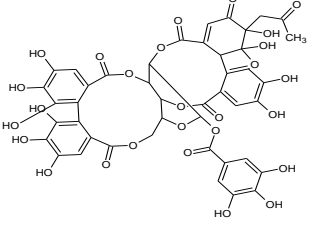
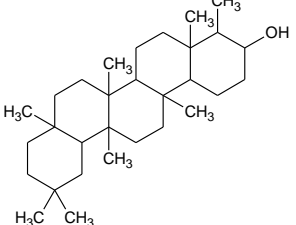
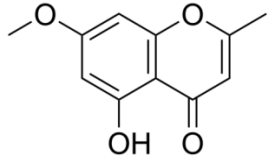
3.2 Target Prediction

The phytochemicals found in *Syzygium cumini* were analyzed using Swiss target prediction database and a total of 243 targets were obtained. An initial search in the Genecards database identified 1386 targets. Potential targets for the management of hyperuricemia were screened using the Venny 2.1.0 platform and 12 overlapping targets were obtained. Out of these, three targets were selected.

3.3 ADMET analysis

The phytochemicals were initially screened through the examination of their pharmacokinetic properties and ADMET analysis. Out of 13 phytochemicals 2-butenic acid, 11-o-galloylbergenin, Betulinic acid, Ellagitannin, Epi-friedelanol, Eugenin, Friedelin, Gallic Acid, Canthaxanthin demonstrated effectiveness. Lipinski's rule of five was also applied to confirm the drug discovery criteria. According to this rule, 6 compounds 2-butenic acid, bergenin, Ellagic acid, Eugenin, Gallic Acid and Kaempferol have zero Lipinski's rule violation, Betulinic acid, epi-friedelanol, friedelin, myricetin have 1 violation, 11-o-galloylbergenin, Canthaxanthin have 2 and Ellagitannin 3 and meet molecular weight of all compounds is < 500 Da except ellagitannin (992.71Da) and canthaxanthin (564.84 Da), Drug Likeness (DL ≥ 0.18), hydrogen bond donors (H donor < 5) except , hydrogen bond acceptors (H acceptor < 10) 11-o-galloylbergenin and ellagitannin and octanol water coefficient (P < 5) except Canthaxanthin (Table 3). An ideal drug is one that adheres to Lipinski's rule without violations [66, 67].

Table 2. Selected Phytochemicals

S.No	Phytochemical name	Structure
1	2-Butenoic acid (PubChem CID: 637090)	
2	11-O-Galloylbergenin (PubChem CID: 56680102)	
3	Bergenin (PubChem CID: 66065)	
4	Betulinic acid (PubChem CID: 64971)	
5	Ellagic acid (PubChem CID: 5281855)	
6	Ellagitannin (PubChem CID: 10033935)	
7	Epi-friedelanol (PubChem CID: 119242)	
8	Eugenin (PubChem CID: 10189)	

Kanaka Raju Addipalli, Aruna Kumari Dokkada, Gana Manjusha K

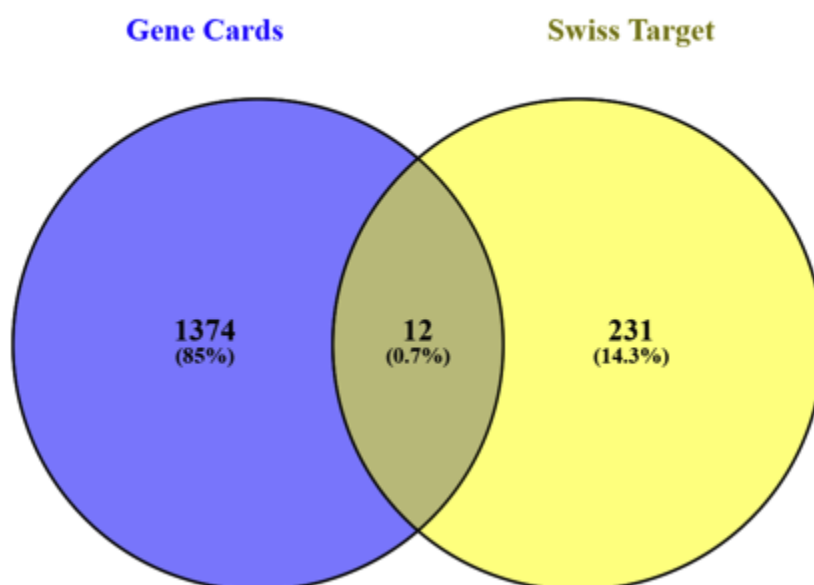
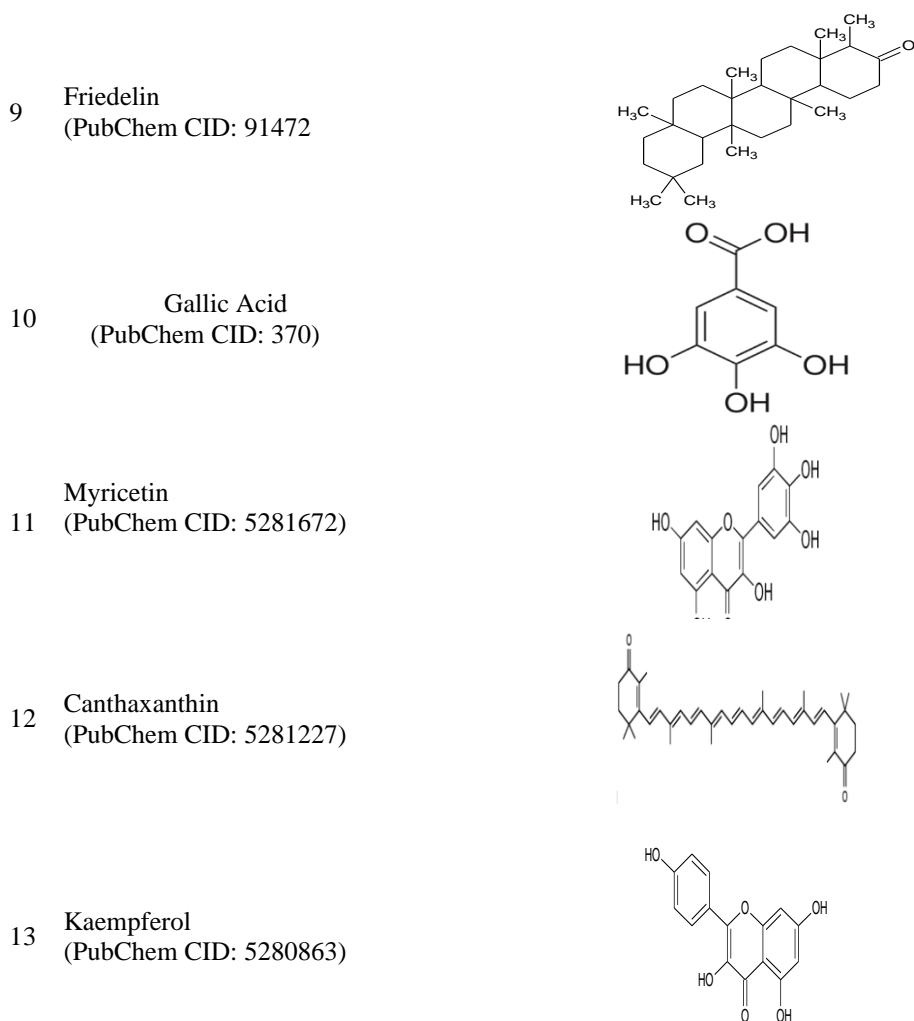


Figure 2. Intersection targets of Phytochemicals and hyperuricemia in *Syzygium cumini* bark

Kanaka Raju Addipalli, Aruna Kumari Dokkada, Gana Manjusha K

Table 3. ADMET Analysis of Selected Phytochemicals

Phytochemical name	MW (<500Da)	Drug likeness	Bioavailability Score	Clog P (<5)	#H-bond acceptors (< 10)	#H-bond donors (< 5)	No of rotatable bonds (< 10)	Total Polar Surface Area	Lipinski Rule of Five violations
2-butenic acid	86.09	1	0.85	0.56	2	1	1	37.3	0
11-O-galloylbergenin	480.38	1	0.17	-0.38	13	7	5	212.67	2
Bergenin	328.27	0	0.55	-0.72	9	5	2	145.91	0
Betulinic acid	456.7	2	0.85	6.13	3	2	2	57.53	1
Ellagic acid	302.19	0	0.55	1	8	4	0	141.34	0
Ellagitannin	992.71	1	0.17	-0.98	27	13	5	447.09	3
Epi-friedelanol	428.73	2	0.55	7.4	1	1	0	20.23	1
Eugenin	206.19	1	0.55	1.89	4	1	1	59.67	0
Friedelin	426.72	2	0.55	7.44	1	0	0	17.07	1
Gallic Acid	170.12	1	0.56	0.21	5	4	1	97.99	0
Myricetin	318.24	0	0.55	0.79	8	6	1	151.59	1
Canthaxanthin	564.84	3	0.17	9.63	2	0	10	34.14	2
Kaempferol	286.24	0	0.55	1.58	6	4	1	111.13	0

Table 4. ADMET analysis of selected phytochemicals

Phytochemical name	CYP1A2 inhibitor	CYP2C19 inhibitor	CYP2C9 inhibitor	CYP2D6 inhibitor	CYP3A4 inhibitor	BBB permeability	Pgp substrate	log Kp (Skin permeation)	GI absorption
2-butenic acid	No	No	No	No	No	Yes	No	-6.31	High
11-O-galloylbergenin	No	No	No	No	No	No	Yes	-9.48	Low
bergenin	No	No	No	No	No	No	No	-8.99	Low
Betulinic acid	No	No	Yes	No	No	No	No	-3.26	Low
Ellagic acid	Yes	No	No	No	No	No	No	-7.36	High
Ellagitannin	No	No	No	No	No	No	Yes	-12.21	Low
Epi-friedelanol	No	No	No	No	No	No	No	-1.76	Low
Eugenin	Yes	No	No	No	No	Yes	No	-5.73	High
Friedelin	No	No	No	No	No	No	No	-1.94	Low
Gallic Acid	No	No	No	No	Yes	No	No	-6.84	High
Myricetin	Yes	No	No	No	Yes	No	No	-7.4	Low
Canthaxanthin	No	No	No	No	No	No	Yes	-1.67	Low
Kaempferol	Yes	No	No	Yes	Yes	No	No	-6.7	High

Kanaka Raju Addipalli, Aruna Kumari Dokkada, Gana Manjusha K

The investigation of ADMET properties for various compounds revealed that four substances, namely 11-o-galloylbergenin, bergenin, betulinic acid, ellagic acid, Ellagitannin, Epi-friedelanol, Friedelin, myricetin Gallic Acid, Canthaxanthin, kaempferol, exhibited an incapacity to penetrate the blood–brain barrier. Conversely, 2-butenic acid and Eugenin demonstrated a high capability to traverse the blood– brain barrier. The blood–brain barrier is a protective barrier formed by endothelial cells in the blood vessels of the brain, which effectively blocks the entry of numerous toxins into brain tissues [68, 69]. Three compounds 11-o-galloylbergenin, Ellagitannin and Canthaxanthin showed positive results for permeability glycoprotein substrates (P-gp substrates) while the remaining compounds showed negative efficacy. The results suggest that non-Pgp substrates exhibit improved persistence in their cells. The role of P-gp in drug transport is essential for pharmacology and drug development, as it can influence the bioavailability and efficacy of various medications [70-72]. In order to maintain consistent plasma concentrations and enhance the absorption of the tested compounds, it was expected that these substances would exhibit inhibitory actions on all five cytochrome P450 enzyme classes, namely CYP2C9, CYP2C19, CYP3A4, CYP1A2, and

CYP2D6. Ellagic acid, Epi-friedelanol, myricetin, kaempferol showed inhibitory effect against CYP1A2, betulinic acid towards CYP2C9 Kaempferol towards CYP2D6, gallic acid, myricetin, kaempferol towards CYP3A4 enzymes. All the compounds showed no inhibitory action against CYP2C19. Cytochrome P450 enzymes are a family of enzymes responsible for metabolizing a wide range of drugs and other xenobiotics (foreign substances) in the body. Inhibiting specific CYP enzymes can enhance drug bioavailability, extend half-life, and mitigate drug-drug interactions [73, 74] (Table 4).

3.3.1. Compound Toxicity Assessment

Toxicity assessment of compounds is a critical step in drug discovery, ensuring the safety and efficacy of potential therapeutic agents. *In silico* tools for molecular docking offer a cost-effective and efficient means to predict drug toxicity, allowing researchers to evaluate potential drug candidates for their safety profiles before advancing to costly *In vitro* and *In vivo* experiments [75, 76]. Compound toxicity was assessed through a comprehensive analysis of six distinct toxicity factors, encompassing mutagenicity, cardiotoxicity, hepatotoxicity, carcinogenicity, Immunotoxicity, and cytotoxicity. (Table 5).

Table 5. Toxicity Prediction of selected phytochemicals

Phytochemical name	Hepatotoxicity	Carcinogenicity	Immunotoxicity	Mutagenicity	Cytotoxicity	Cardiotoxicity
2-Butenoic acid	Inactive	Inactive	Inactive	Inactive	Inactive	Inactive
11-o-galloylbergenin	Inactive	Inactive	Active	Active	Inactive	Active
Bergenin	Inactive	Inactive	Active	Inactive	Inactive	Inactive
Betulinic acid	Inactive	Active	Active	Inactive	Inactive	Active
Ellagic acid	Inactive	Active	Inactive	Inactive	Inactive	Inactive
Ellagitannin	Inactive	Inactive	Active	Inactive	Inactive	Inactive
Epi-friedelanol	Inactive	Inactive	Inactive	Inactive	Inactive	Inactive
Eugenin	Inactive	Active	Inactive	Active	Inactive	Inactive
Friedelin	Inactive	Inactive	Active	Inactive	Inactive	Inactive
Gallic Acid	Inactive	Active	Inactive	Inactive	Inactive	Inactive
Myricetin	Inactive	Active	Inactive	Active	Inactive	Inactive
Canthaxanthin	Inactive	Inactive	Inactive	Inactive	Inactive	Inactive
Kaempferol	Inactive	Inactive	Inactive	Inactive	Inactive	Inactive

Table 6. Predicted LD 50 of selected phytochemicals

S.No	Phytochemical name	Predicted LD ₅₀	Predicted Toxicity Class
1	2-Butenoic acid	1000mg/kg	Class IV
2	11-O-galloylbergenin	10000mg/kg	Class VI
3	bergenin	10000mg/kg	Class VI

Kanaka Raju Addipalli, Aruna Kumari Dokkada, Gana Manjusha K

4	Betulinic acid	2610mg/kg	Class VI
5	Ellagic acid	2991mg/kg	Class IV
6	Ellagitannin	620mg/kg	Class IV
7	Epi-friedelanol	940mg/kg	Class IV
8	Eugenin	100mg/kg	Class III
9	Friedelin	500mg/kg	Class IV
10	Gallic Acid	2000mg/kg	Class IV
11	myricetin	159mg/kg	Class III
12	Canthaxanthin	10000mg/kg	Class VI
13	Kaempferol	3919mg/kg	Class VI

Table 7. Prediction of interacting residues for selected proteins using CASTp

S.no	Protein name	Interacting residues (predicted by CASTp)
1	Xanthine oxidase	LEU-245,LYS-249,PRO-253,ALA-255,LYS-256,LEU257,VAL258,VAL-259,GLY-260,ASN-261,THR-262,,GLU-263,ILE-264,ILE-266,GLU267,PHE-270,LYS-271,GLN-273,PRO-281,LEU-287,ALA301,ALA-302,LEU-305,PHE-337,ALA-338,VAL-342,ALA-346,SER,347,GLY-349,GLY-350,ASN-351,ILE-353,THR-354,SER-354,ILE-358,SER-359,ASP-360,TYR-393,ARG-394,THR-396,LEU-398,GLY-399,PRO-400,GLU-402,ILE-403,LEU-404,LYS422,ARG-426,ASP-429,ASP-430,LYS-433 CYS-65, VAL-66,LEU-67,LYS-68,GLY-69,GLY-70,TYR-71,LYS-72,PHE-73,PHE-74,ARG-100,LEU-101,LYS-102,SER-103,TYR-104,CYS-105,SER-109,THR-110, ASP-112,ILE-113,LYS-114,VAL-132,GLU-133,ASP-134,ILE-135,ILE-136,ASP-137,THR-138,GLY-139,LYS140,THR-141,MET-142,LYS-165,PHE-186,VAL-187,VAL-188,GLY-189,TYR-190,ALA-191,LEU-192,ASP-193,TYR-194,ASN-195,GLU-196,PHE-198,ARG-199,LEU-201,ALA-217
2	HGPRT	HIS-17,ASP-19,MET-52,LEU-56,THR-57,LEU-58,PHE-61,LEU-62,PHE-65,TYR-102,SER-103,LEU-106,TRP-117,CYS-153,MET-155,ARG-156,HIS-157,ALA-183,GLY-184,ASP-185,GLU-186,THR-187,HIS-214GLU-217,VAL-218,HIS-258,SER-265,LEU-268,THR-269,ASP-295,ASP-296,PHE-300
3	Adenosine deaminase	

3.3.2 Prediction of LD50 and drug class

The level of toxicity varies according to the dosage, the short-term toxic impact is assessed through the median lethal dose (LD50) [77]. Compounds LD50 and toxicity class prediction results showed that five compounds 11-o-galloylbergenin, bergenin, betulinic acid, canthaxanthin, kaempferol have drug toxicity class VI (LD₅₀ = 10000 mg/kg, LD₅₀ = 10000 mg/kg, LD₅₀ = 2610 mg/kg, LD₅₀ = 10000 mg/kg, LD₅₀ = 3919 mg/kg respectively), which are non toxic; six compounds 2-butenic acid, ellagic acid, ellagitannin, epi-friedelanol , friedelin, Gallic Acid have drug toxicity class IV (LD₅₀ = 1000 mg/kg, LD₅₀ = 2991 mg/kg, LD₅₀ = 620 mg/kg, LD₅₀ = 940 mg/kg, LD₅₀ = 500 mg/kg, LD₅₀ = 2000 mg/kg) can be harmful if swallowed; and two compounds eugenin and myricetin have drug toxicity class III (LD₅₀ = 100 mg/kg and LD₅₀ =

159 mg/kg, respectively), can be toxic if swallowed (Table 6)

Class I: fatal if swallowed (LD₅₀ ≤ 5); Class II: fatal if swallowed (5 < LD₅₀ ≤ 50); Class III: toxic if swallowed (50 < LD₅₀ ≤ 300); Class IV: harmful if swallowed (300 < LD₅₀ ≤ 2000); Class V: may be harmful if swallowed (2000 < LD₅₀ ≤ 5000); Class VI: non-toxic (LD₅₀ > 5000)

3.4 Molecular docking study

3.4.1 Active site prediction

The active site prediction for three selected proteins was conducted using the CASTp server. The interacting residues within the binding pocket, which has a large surface area and volume, are presented in the table. 7 and figure 3.

Kanaka Raju Addipalli, Aruna Kumari Dokkada, Gana Manjusha K

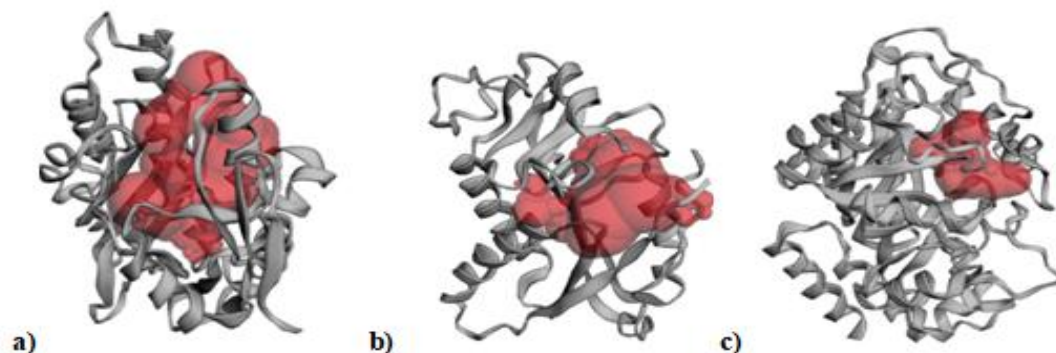


Figure 3. The active sites of (a) Xanthine oxidase, (b) HGPRT, and (c) Adenosine deaminase were predicted using the CASTp server, with the binding pockets represented as red-colored spheres.

Table 8. Binding energy of thirteen ligands with three proteins

S.No	Phytochemical name	Binding energy (K.cal/mol)		
		Xanthine oxidase	HGPRT	Adenosine deaminase
1	2-Butenoic acid	-4.4	-4.5	-4.2
2	11-O-galloylbergenin	-10.8	-8.3	-8.7
3	Bergenin	-9.2	-6.5	-7.7
4	Betulinic acid	-7.7	-7.6	-7.1
5	Ellagic acid	-8	-7.8	-7.8
6	Ellagitannin	-8.8	-9.7	-8.2
7	Epi-friedelanol	-8.5	-7.8	-7.4
8	Eugenin	-5.7	6.8	-6.4
9	Friedelin	-9.1	-7.8	-7.8
10	Gallic acid	-6.5	-5.6	-5.6
11	Myricetin	-9	-8.6	-9
12	Canthaxanthin	-8.7	-7.3	-11.1
13	Kaempferol	-8.9	-8.1	-6.6

1

3.4.2 Docking analysis

Docking study of thirteen ligands with three proteins—Xanthine oxidase, HGPRT, and Adenosine deaminase produces varying binding energies, listed in table 8. Among the thirteen ligands, the four with the higher negative binding energies for these proteins were selected for further docking studies. The binding energy, number of hydrogen bonds, residual interactions of top four ranked ligands is detailed in Table 9. The docking poses of the top four ranked ligands forming complexes with Xanthine oxidase, HGPRT, and Adenosine deaminase are also represented in figure 3,4,5.

3.4.3 Docking study of ligands with Xanthine oxidase

When thirteen ligands subjected to docking with Xanthine oxidase, four ligands shows highest negative binding energy are 11-O-galloylbergenin,

Bergenin, Friedelin and Myricetin. Among top four ranked ligands 11-O-galloylbergenin shows the most favourable binding energy of -10.8 kcal/mol, indicating it forms the most stable complex with Xanthine oxidase. The higher negative binding energy reflects stronger interactions and potential inhibitory effects on the protein, 11-o-galloylbergenin forms the five hydrogen bonds with protein and key residues involved in hydrogen bonding are GLU-263, ASN-351, THR-357, SER-347 and LEU-404 are also highlighted. Bergenin follows with a binding energy of -9.2 kcal/mol, forms three hydrogen bonds with protein and key residues involved in hydrogen bonding are GLY-260, ASN-261 and SER-347.

Kanaka Raju Addipalli, Aruna Kumari Dokkada, Gana Manjusha K

S.No	Protein name	Phytochemical name	Binding energy (Kcal/mol)	No of hydrogen bonds	Conventional hydrogen bond	Pi-Pi/Pi-alkyl/Pi-sigma	Van der waals
1	Xanthine oxidase	11-O-galloylbergenin	-10.8	5	GLU-263, ASN-351, THR-357, SER-347, LEU-404	GLY-350., ILE- 353, LEU-257, PRO-281, ALA-302, ALA-301, VAL-259	PHE-337, LEU-305, ILE-264, LYS-256, GLY-260, ASN-261, ALA-346, GLY-349, ILE-403
		Bergenin	-9.2	3	GLY-260, ASN-261, SER-347	LEU-257, ILE-353	GLY-265, THR-262, ALA,346, VAL-259, GLY-350, ALA-302, ALA-301, GLY-349, LEU-404, ILE-403, LYS-256, LEU-398, GLU-263
		Friedelin	-9.1	1	ARG-233	PHE-229, TRP-236	GLU-232, GLY-231, LEU-274, VAL-234, MET-268, ILE-278
		Myricetin	-9	4	LYS-256, ASN-261, GLY-260, VAL-259	LEU-257, ILE-353, ILE-264	GLY-350, THR-354, THR-262, VAL-258, LEU-404, LEU-398, ILE-403
2	HGPRT	Ellagitannin	-9.7	6	PHE-186, ARG-169, THR-138, LYS-165, ASP-193, GLU-133	THR-110	LYS-212, SER-103, LYS-185, ASP-184, GLN-108, MET-142, LYS-140, ILE-136, THR-141, VAL-187, LEU-192, GLY-69,
		Myricetin	-8.6	3	THR-141, THR-138, VAL-187,	ILE-135, PHE-186	LYS-165, ILE-136, MET-142, LYS-140,

Kanaka Raju Addipalli, Aruna Kumari Dokkada, Gana Manjusha K

							ASP-137, ARG-169, LYS-68, ASP-193
		11-O-galloylbergenin	-8.3	3	LYS-102, SER-109, GLY-69	LEU-192, ILE-135	ALA-191, ASP-193, VAL-187, PHE-186, LYS-165, ASP-137, THR-138, THR-110, GLN-108, CYS-105, ASP-112, ILE-113, LYS-114, LEU-101, SER-103
		Kaempferol	-8.1	1	THR-141	THR-110, ILE-135, PHE-186	LYS-68, THR-138, LYS-140, GLY-139, ILE-136, ASP-137, LYS-165, LYS-185, VAL-187, ASP-193
3	Adenosine deaminase	Canthaxanthin	-11.1	Nil	NIL	HIS-17, TRP-117, PHE-65, LEU-62, LEU-106	GLY-184, PHE-61, LEU-56, THR-269, THR-57, VAL-218, THR-187, GLU-186, LEU-58, ASP-185, ASN-118, PRO-114, ILE-115, PRO-116, MET-155, ASP-19, ASP-296,
		Myricetin	-9	3	HIS-17, ASP-295, LEU-56	LEU-58, VAL-218	HIS-214, ASP-296, PHE-65, LEU-62, PHE-61, THR-269, THR-57, THR-187, ASP-185, GLU-186, GLY-184

Kanaka Raju Addipalli, Aruna Kumari Dokkada, Gana Manjusha K

		11-O-galloylbergenin	-8.7	4	TRP-117, ASP-19, GLU-217, ASP-185	LEU-62, PHE-65, HIS-17, PHE-61, LEU-58	ASP-66, PRO-116, HIS-157, MET-155, LEU-106, ASP-296, THR-269
		Ellagitannin	-8.2	5	ASN-289, GLY-208, GLU-337, GLU-255, LYS-340	HIS-210	HIS-258, LYS-331, GLU-234, VAL-209, ARG-173, PRO-336, LYS-341, SER-333, PHE-334, SER-332,

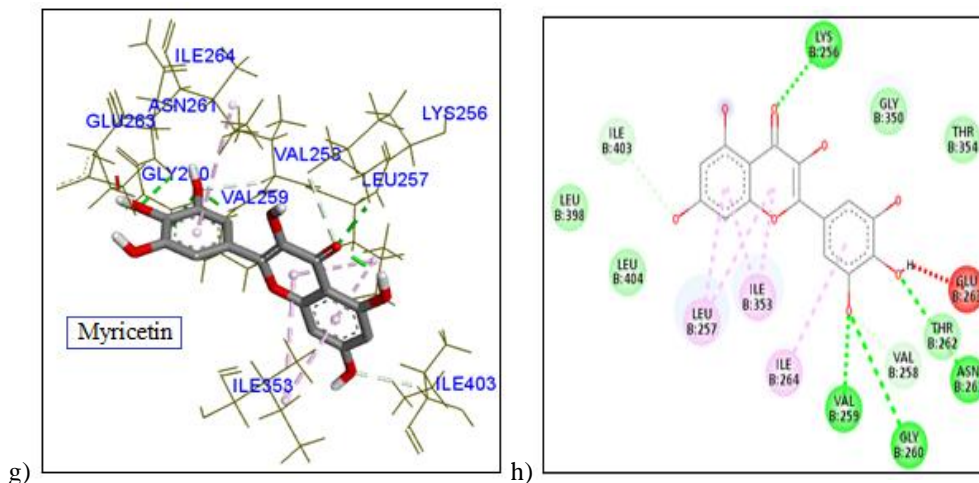
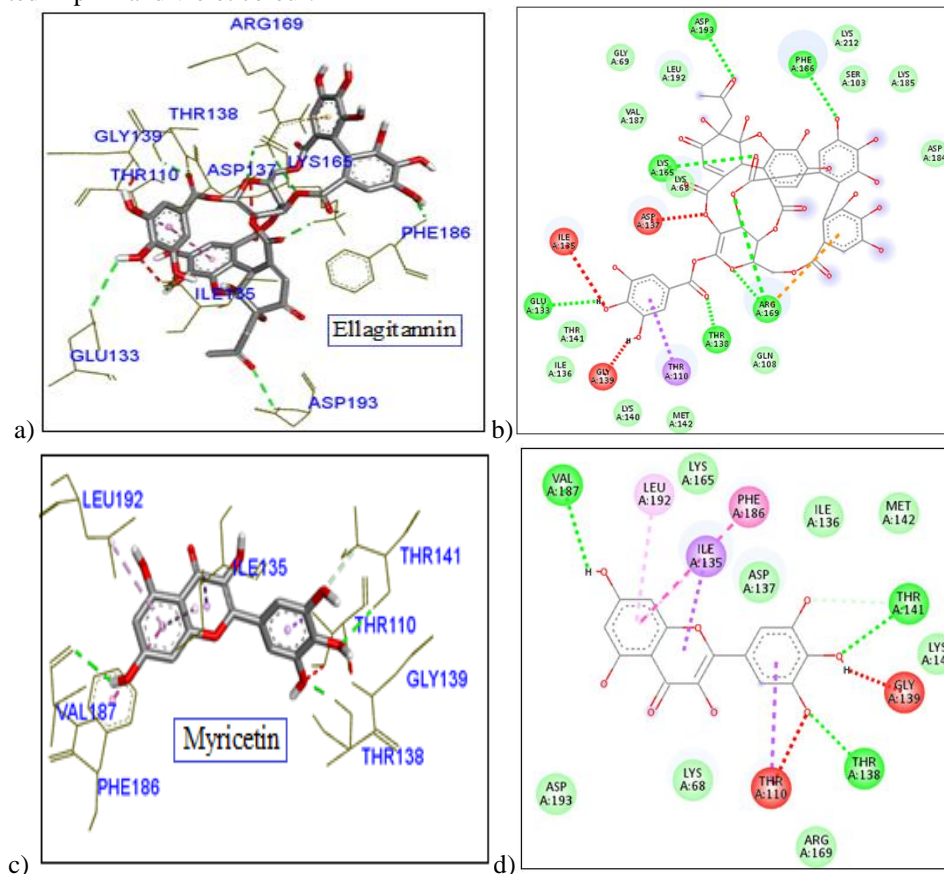


Figure 4. (a) - (h) Binding interactions of the top 4 ranked ligands 11-o-galloyl bergenin, Bergenin, Friedelin and Myricetin at the active site of xanthine oxidase along with their 2-D interactions. The interacting residues of protein represented as lines in green colour and the ligands represented in grey colour stick model. The conventional hydrogen bonds represented in green colour and non covalent interactions represented in pink and violet colour.



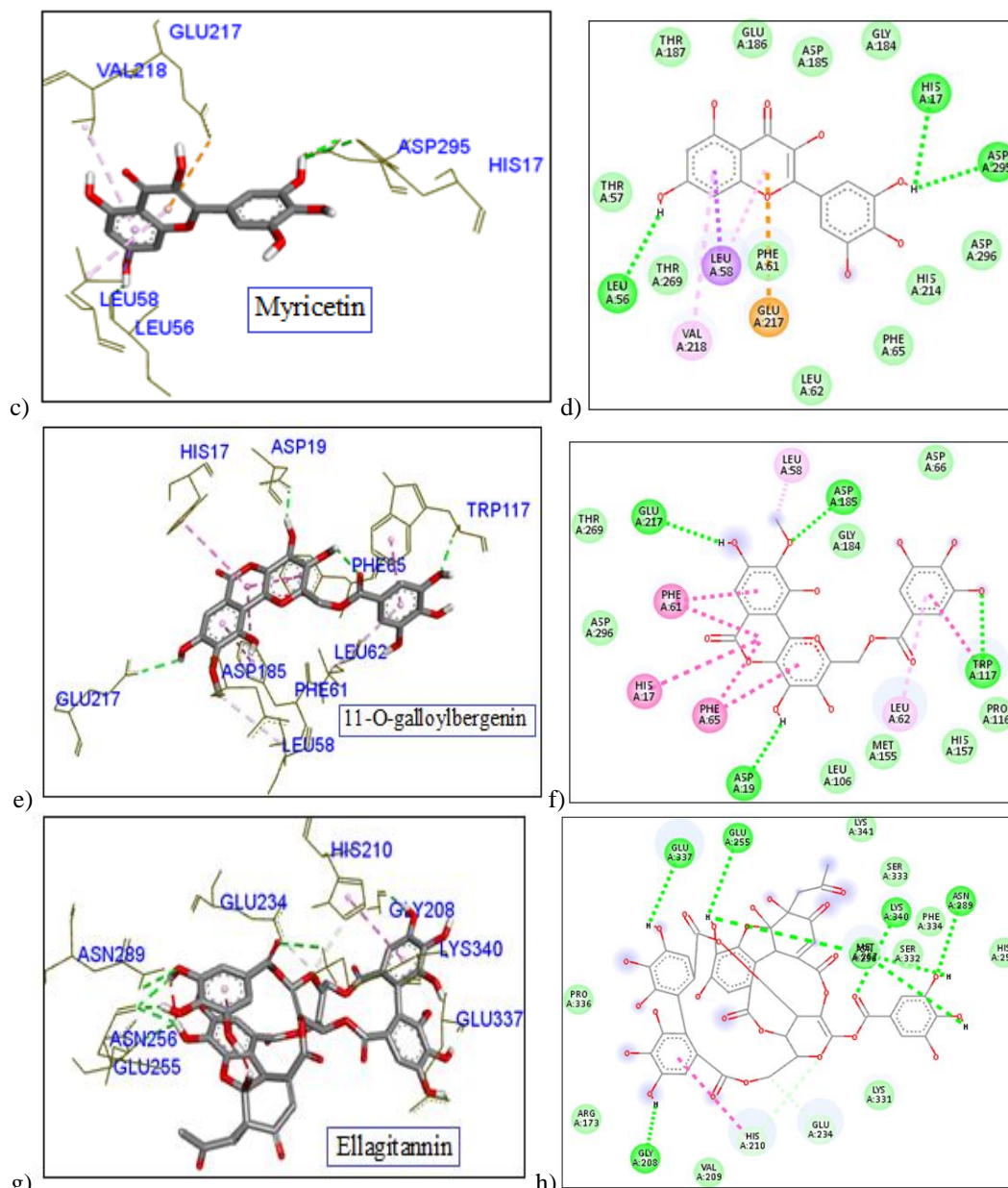


Figure 6. (a) - (h) Binding interactions of the top 4 ranked ligands Canthaxanthin, Myricetin, 11-o-galloyl bergenin and Ellagitannin at the active site of Adenosine deaminase along with their 2-D interactions. The interacting residues of protein represented as lines in green colour and the ligands represented in grey colour stick model. The conventional hydrogen bonds represented in green colour and non covalent interactions represented in pink and violet colour.

While Friedelin and Myricetin shows slightly weaker binding affinities with energies of -9.1 kcal/mol and -9 kcal/mol, Friedelin form one hydrogen bond with protein and key residue involved is ARG-233 and Myricetin forms four hydrogen bonds with protein, key residues involved in hydrogen bonding are LYS-256, ASN-261, GLY-260, VAL-259. The docking results suggest that 11-o-galloylbergenin is the strongest binder to xanthine oxidase due to its highest negative binding

energy, higher number of hydrogen bonds, and more extensive residual interactions. The combination of strong hydrogen bonding, Pi-Pi interactions, and Van der Waals forces enhances the stability of the complex, making it a promising candidate for inhibiting xanthine oxidase activity. While Bergenin, Friedelin and Myricetin also shows favourable binding, with a moderately strong interaction profile exhibit inhibitory effects due to their significant interactions with key residues.

3.4.4 Docking study of ligands with HGPRT

When thirteen ligands subjected to docking with HGPRT, four ligands shows highest negative binding energy are Ellagitannin, Myricetin, 11-O-galloylbergenin and Kaempferol. Among top four ranked ligands Ellagitannin shows the most favourable binding energy of -9.7 kcal/mol, indicating it forms the most stable complex with HGPRT. The higher negative binding energy reflects stronger interactions and potential inhibitory effects on the protein, Ellagitannin forms the six hydrogen bonds with protein and key residues involved in hydrogen bonding are PHE-186, ARG-169, THR-138, LYS-165, ASP-193 and GLU-133 are also highlighted. Myricetin and 11-o-galloylbergenin shows moderately binding energies of -8.6 kcal/mol and -8.3 kcal/mol respectively. Myricetin form three hydrogen bonds with protein, key residues involved in hydrogen bonding are THR-141, THR-138, and VAL-187 and 11-o-galloylbergenin forms three hydrogen bonds with protein, key residues involved in hydrogen bonding are LYS-102, SER-10 and GLY-69. While Kaempferol shows the weakest binding energy (-8.1 kcal/mol) and forms only 1 hydrogen bond, key residue involved in hydrogen bonding is THR-141. The docking results suggest that Ellagitannin is the strongest binder to HGPRT due to its highest negative binding energy, higher number of hydrogen bonds, and more extensive residual interactions. The combination of strong hydrogen bonding, Pi-Pi interactions, and Van der Waals forces enhances the stability of the complex, making it a promising candidate for inhibiting HGPRT. Myricetin and 11-O-galloylbergenin also shows favourable binding with a moderately strong interaction profile, while Kaempferol have relatively weaker binding but may still exhibit inhibitory effects due to their significant interactions with key residues.

3.4.5 Docking study of ligands with Adenosine deaminase

When thirteen ligands subjected to docking with Adenosine deaminase, four ligands shows highest negative binding energy are Canthaxanthin, Myricetin, 11-O-galloylbergenin and Ellagitannin. Among top four ranked ligands Canthaxanthin shows the most favorable binding energy of -11.1 kcal/mol, indicating it forms the most stable complex with Adenosine deaminase. The higher

negative binding energy reflects stronger interactions and potential inhibitory effects on the protein, Canthaxanthin forms no hydrogen bonds, which is unusual for highest negative binding energy. The stability of its complex with adenosine deaminase likely arises from extensive hydrophobic interactions and Van der Waals forces. Myricetin shows moderately binding energy of -9 kcal/mol, forms three hydrogen bonds with protein and key residues involved in hydrogen bonding are HIS-17, ASP-295 and LEU-56. 11-o-galloylbergenin shows a binding energy of -8.7 kcal/mol, forms four hydrogen bonds with protein and key residues involved in hydrogen bonding are TRP-117, ASP-19, GLU-217 and ASP-185. While Ellagitannin shows the weakest binding energy -8.2 kcal/mol, forms extensively five hydrogen bonds and key residues involved in hydrogen bonding are ASN-289, GLY-208, GLU-337, GLU-255 and LYS-340. The docking results reveal that Canthaxanthin binds most strongly to adenosine deaminase, as indicated by its highly negative binding energy. The lack of hydrogen bonds implies that its binding is predominantly driven by hydrophobic interactions and Van der Waals forces, rather than specific electrostatic interactions. Myricetin, 11-o-galloylbergenin, and Ellagitannin exhibit moderately strong binding to the enzyme, with binding energies between -9 kcal/mol and -8.2 kcal/mol. Their stability is largely attributed to the formation of multiple hydrogen bonds, especially for Ellagitannin and 11-o-galloylbergenin, which show more extensive bonding with key residues in the protein active site.

4. Conclusions

The findings from this study highlight the therapeutic potential of phytochemicals derived from *Syzygium cumini* bark, particularly for managing hyperuricemia. Through target prediction, ADMET analysis, and molecular docking, we identified 11-O-galloylbergenin and other bioactive compounds that show promise as effective inhibitors of enzymes associated with hyperuricemia. The favourable pharmacokinetic and safety profiles of these compounds underscore their potential as natural alternatives to synthetic drugs. This study provides a valuable insight into the drug-likeness and efficacy of *S. cumini*'s phytochemicals, encouraging further research into their development as targeted therapeutics. Future investigations are warranted to validate these

findings *in vivo*, facilitating the transition from natural compound screening to clinical applications. The molecular docking study provides insights into the binding affinities and interaction profiles of various phytochemicals with Xanthine oxidase, HGPRT, and Adenosine deaminase, enzymes integral to oxidative stress and hyperuricemia. 11-o-galloylbergenin exhibited the most favourable binding to Xanthine oxidase, forming multiple hydrogen bonds and contributing to complex stability through Pi-Pi interactions. Ellagitannin showed strong binding with HGPRT, with extensive hydrogen bonding enhancing its inhibitory potential. Similarly, Canthaxanthin displayed the highest binding affinity to Adenosine deaminase, primarily driven by hydrophobic interactions and Vander Waals forces. These findings suggest that 11-o-galloylbergenin, Ellagitannin, and Canthaxanthin hold promise as potential inhibitors for these enzymes. Further *in vitro* and *in vivo* studies are warranted to explore these phytochemicals' therapeutic potential in managing oxidative stress and uric acid-related disorders.

ACKNOWLEDGEMENT

The facilities required to conduct this research were provided by Prof. Y Srinivasa Rao, Principal, Vignan Institute of Pharmaceutical Technology, and Lavu Educational Society, for which the authors are grateful.

References

- [1] L. Li, Y. Zhang, C. Zeng, Update on the epidemiology, genetics, and therapeutic options of hyperuricemia, *Am J Transl Res* 12 (2020) 3167–3181.
- [2] L. Du, Y. Zong, H. Li, et al., Hyperuricemia and its related diseases: mechanisms and advances in therapy, *Sig Transduct Target Ther* 9 (2024) 212.
- [3] J. Song, et al., Prevalence and risk factors of hyperuricemia and gout: a cross-sectional survey from 31 provinces in mainland China, *J Transl Intern Med* 10 (2022) 134–145.
- [4] E. Alemayehu, et al., Prevalence of hyperuricemia among type 2 diabetes mellitus patients in Africa: a systematic review and meta-analysis, *BMC Endocr Disord* 23 (2023) 153.
- [5] E. Adomako, O.W. Moe, Uric acid and urate in urolithiasis: the innocent bystander, instigator, and perpetrator, *Semin Nephrol* 40 (2020) 564–573.
- [6] J. Maiuolo, F. Oppedisano, S. Gratteri, C. Muscoli, V. Mollace, Regulation of uric acid metabolism and excretion, *Int J Cardiol* 213 (2016) 8–14.
- [7] M. Jin, F. Yang, I. Yang, Y. Yin, J.J. Luo, H. Wang, X.F. Yang, Uric acid, hyperuricemia and vascular diseases, *Front Biosci (Landmark Ed)* 17 (2012) 656–669.
- [8] X.W. Wu, D.M. Muzny, C.C. Lee, C.T. Caskey, Two independent mutational events in the loss of urate oxidase during hominoid evolution, *J Mol Evol* 34 (1992) 78–84.
- [9] G. Desideri, G. Castaldo, A. Lombardi, et al., Is it time to revise the normal range of serum uric acid levels?, *Eur Rev Med Pharmacol Sci* 18 (2014) 1295–1306.
- [10] J. Su, Y. Wei, M. Liu, et al., Anti-hyperuricemic and nephroprotective effects of *Rhizoma Dioscoreae septemlobae* extracts and its main component dioscin via regulation of mOAT1, mURAT1 and mOCT2 in hypertensive mice, *Arch Pharm Res* 37 (2014) 1336–1344.
- [11] K. Chaudhary, K. Malhotra, J. Sowers, A. Aroor, Uric acid — key ingredient in the recipe for cardiorenal metabolic syndrome, *Cardiorenal Med* 3 (2013) 208–220.
- [12] M. Jin, F. Yang, I. Yang, et al., Uric acid, hyperuricemia and vascular diseases, *Front Biosci* 17 (2012) 656–669.
- [13] X.H. Wu, J. Zhang, S.Q. Wang, V.C. Yang, S. Anderson, Y.W. Zhang, Riparoside B and timosaponin J, two steroidal glycosides from *Smilax riparia*, resist hyperuricemia based on URAT1 in hyperuricemic mice, *Phytomedicine* 21 (2014) 1196–1201.
- [14] H. Matsuo, A. Nakayama, M. Sakiyama, et al., ABCG2 dysfunction causes hyperuricemia due to both renal urate underexcretion and renal urate overload, *Sci Rep* 4 (2014) 3755.
- [15] D.B. Mandal, Mount, The molecular physiology of uric acid homeostasis, *Annu Rev Physiol* 77 (2014) 323–345.
- [16] B.P. Cléménçon, M. Lüscher, G. Fine, et al., Expression, purification, and structural

- insights for the human uric acid transporter, GLUT9, using the *Xenopus laevis* oocytes system, *PLoS One* 9 (2014).
- [17] N. Cantu-Medellin, E.E. Kelley, Xanthine oxidoreductase-catalyzed reactive species generation: a process in critical need of reevaluation, *Redox Biol* 1 (2013) 353–358.
- [18] C.M. Harris, V. Massey, The action of reduced xanthine dehydrogenase with molecular oxygen. Reaction kinetics and measurement of superoxide radical, *J Biol Chem* 272 (1997) 8370–8379.
- [19] C. Beedham, Xanthine oxidoreductase and aldehyde oxidase, in: C.A. McQueen (Ed.), *Comprehensive Toxicology*, 4th ed., 2010, pp. 185–205.
- [20] T. Iwasaki, K. Okamoto, T. Nishino, J. Mizushima, H. Hori, Sequence motif-specific assignment of two [2Fe–2S] clusters in rat xanthine oxidoreductase studied by site-directed mutagenesis, *J Biochem* 127 (2000) 771–778.
- [21] C.E. Berry, J.M. Hare, Xanthine oxidoreductase and cardiovascular disease: molecular mechanisms and pathophysiological implications, *J Physiol* 555 (2004) 589–606.
- [22] K. Schröder, C. Vecchione, O. Jung, et al., Xanthine oxidase inhibitor tungsten prevents the development of atherosclerosis in ApoE knockout mice fed a Western-type diet, *Free Radic Biol Med* 41 (2006) 1353–1360.
- [23] Z.W. Zhang, Q.H. Wang, J.L. Zhang, S. Li, X.L. Wang, S.W. Xu, Effects of oxidative stress on immunosuppression induced by selenium deficiency in chickens, *Biol Trace Elem Res* 149 (2012) 352–361.
- [24] F. Stirpe, M. Ravaiol, M.G. Battelli, S. Musini, G.L. Grazi, Xanthine oxidoreductase activity in human liver disease, *Am J Gastroenterol* 97 (2002) 2079–2085.
- [25] M. Sakela, R. Lapatto, K.O. Raivio, Xanthine oxidoreductase gene expression and enzyme activity in developing human tissues, *Biol Neonate* 74 (1998) 274–280.
- [26] N. Dalbeth, L.K. Stamp, Chapter 13 - Xanthine Oxidase Inhibitor Treatment of Hyperuricemia, *Gout & Other Crystal Arthropathies*, W.B. Saunders, 2012, pp. 154–173.
- [27] J.T. Hancock, V. Salisbury, M.C. Ovejero-Boglione, R. Cherry, R. Eisenthal, R. Harrison, Antimicrobial properties of milk: dependence on presence of xanthine oxidase and nitrite, *Antimicrob Agents Chemother* 46 (2002) 3308–3310.
- [28] B.L.J. Godber, J.J. Doel, J. Durgan, R. Eisenthal, R. Harrison, A new route to peroxyxynitrite: a role for xanthine oxidoreductase, *FEBS Lett* 475 (2000) 93–96.
- [29] M. Jin, F. Yang, I. Yang, et al., Uric acid, hyperuricemia and vascular diseases, *Front Biosci* 17 (2012) 656–669.
- [30] H.A. Jinnah, Lesch–Nyhan disease and its variants, in: *Reference Module in Neuroscience and Biobehavioral Psychology*, Elsevier, 2017.
- [31] L. Antonioli, R. Colucci, C. La Motta, M. Tuccori, O. Awwad, F. Da Settimo, C. Blandizzi, M. Fornai, Adenosine deaminase in the modulation of the immune system and its potential as a novel target for treatment of inflammatory disorders, *Curr Drug Targets* 13 (2012) 842–862.
- [32] Atta, M.M. Salem, K.S. El-Said, T.M. Mohamed, Mechanistic role of quercetin as inhibitor for adenosine deaminase enzyme in rheumatoid arthritis: systematic review, *Cell Mol Biol Lett* 29 (2024) 14. <https://doi.org/10.1186/s11658-024-00531-7>.
- [33] E. Cortés, E. Gracia, M. Moreno, et al., Moonlighting adenosine deaminase: a target protein for drug development, *Med Res Rev* 35 (2015) 85–125.
- [34] E. Gracia, K. Pérez-Capote, E. Moreno, et al., A2A adenosine receptor ligand binding and signalling is allosterically modulated by adenosine deaminase, *Biochem J* 435 (2011) 701–709.
- [35] S.G. Mallat, S. Al Kattar, B.Y. Tanios, A. Jurjus, Hyperuricemia, hypertension, and chronic kidney disease: an emerging association, *Curr Hypertens Rep* 18 (2016) 74.
- [36] M. Mazzali, J. Hughes, Y.G. Kim, et al., Elevated uric acid increases blood pressure in the rat by a novel crystal-independent mechanism, *Hypertension* 38 (2001) 1101–1106.

- [37] M. Mazzali, J. Kanellis, L. Han, et al., Hyperuricemia induces a primary renal arteriolopathy in rats by a blood pressure-independent mechanism, *Am J Physiol Renal Physiol* 282 (2002) F997–F1003.
- [38] L.G. Sanchez-Lozada, E. Tapia, C. Avila-Casado, et al., Mild hyperuricemia induces glomerular hypertension in normal rats, *Am J Physiol Renal Physiol* 283 (2002) F1105–F1110.
- [39] D.H. Kang, T. Nakagawa, L. Feng, et al., A role for uric acid in the progression of renal disease, *J Am Soc Nephrol* 13 (2002) 2888–2897.
- [40] L.G. Sanchez-Lozada, E. Tapia, J. Santamaria, et al., Mild hyperuricemia induces vasoconstriction and maintains glomerular hypertension in normal and remnant kidney rats, *Kidney Int* 67 (2005) 237–247.
- [41] L.G. Sanchez-Lozada, M.A. Lanasa, M. Cristobal-Garcia, et al., Uric acid-induced endothelial dysfunction is associated with mitochondrial alterations and decreased intracellular ATP concentrations, *Nephron Exp Nephrol* 121 (2012) e78–e86
- [42] G. Zoppini, G. Targher, M. Chonchol, et al., Serum uric acid levels and incident chronic kidney disease in patients with type 2 diabetes and preserved kidney function, *Diabetes Care* 35 (2012) 99–104.
- [43] U.M. Khosla, S. Zharikov, J.L. Finch, et al., Hyperuricemia induces endothelial dysfunction, *Kidney Int.* 67 (2005) 1739–1742.
- [44] C.A. Farquharson, R. Butler, A. Hill, J.J. Belch, A.D. Struthers, Allopurinol improves endothelial dysfunction in chronic heart failure, *Circulation* 106 (2002) 221–226.
- [45] R. Butler, A.D. Morris, J.J. Belch, A. Hill, A.D. Struthers, Allopurinol normalizes endothelial dysfunction in type 2 diabetics with mild hypertension, *Hypertension* 35 (2000) 746–751.
- [46] T. Nakagawa, M. Mazzali, D.H. Kang, et al., Hyperuricemia causes glomerular hypertrophy in the rat, *Am J Nephrol.* 23 (2003) 2–7.
- [47] E.S. Ryu, M.J. Kim, H.S. Shin, et al., Uric acid-induced phenotypic transition of renal tubular cells as a novel mechanism of chronic kidney disease, *Am J Physiol Renal Physiol.* 304 (2013) F480.
- [48] D-D. Kim, J-J. Hwang, Uric acid and cardiovascular disease: A clinical review, *Korean J Intern Med.* 36 (2021) 934–945. doi: 10.3904/kjim.2020.410.
- [49] S. Sidana, V.B. Singh, Effect of *Syzygium cumini* (Jamun) seed powder on blood pressure in patients with type 2 diabetes mellitus – a double-blind randomized control trial, *Int J Sci Res.* 5 (2016) 753–755.
- [50] T. Cavatão de Freitas, R.J. Oliveira, R.J. Mendonça, Identification of bioactive compounds and analysis of inhibitory potential of the digestive enzymes from *Syzygium* sp. extracts, *J Chem.* 2019 (2019) 3410953.
- [51] M. Qamar, S. Akhtar, T. Ismail, et al., *Syzygium cumini* (L.) Skeels fruit extracts: *In vitro* and *in vivo* anti-inflammatory properties, *J Ethnopharmacol.* 271 (2021) 113805.
- [52] Siddika, P.K. Das, S.Y. Asha, et al., Antiproliferative Activity and Apoptotic Efficiency of *Syzygium cumini* Bark Methanolic Extract against EAC Cells *In Vivo*, *Anticancer Agents Med Chem.* 21 (2021) 782–792.
- [53] M. Qamar, S. Akhtar, T. Ismail, et al., Phytochemical Profile, Biological Properties, and Food Applications of the Medicinal Plant *Syzygium cumini*, *Foods* 11 (2022) 378.
- [54] S. Tantratian, W. Krusong, O. Siriwetwut, Combination of *Syzygium cumini* (L) Skeels seed extract with acetic acid to control *Escherichia coli* on mint (*Mentha cordifolia* opiz.) leaves, *Lebensm Wiss Technol.* 164 (2022) 113619.
- [55] D. Zhang, Q. Zhou, Z. Zhang, et al., Based on Network Pharmacology and Molecular Docking, the Active Components, Targets, and Mechanisms of *Flemingia philippinensis* in Improving Inflammation Were Excavated, *Nutrients* 16 (2024) 1850.
- [56] J. Liu, J-L. Shi, J-Y. Guo, et al., Anxiolytic-like effect of Suanzaoren-Wuweizi herb-pair and evidence for the involvement of the monoaminergic system in mice based on network pharmacology, *BMC Complement Med Ther.* 23 (2023) 7

- [57] Shahzadi, Z., Yousaf, Z., Anjum, I., et al. (2024). Network pharmacology and molecular docking: combined computational approaches to explore the antihypertensive potential of *Fabaceae* species. *Bioresources and Bioprocessing*, 11(1), 53.
- [58] Nafisah, W., Fatchiyah, F., Widyananda, M. H., Christina, Y. I., Rifai, M., Widodo, N., & Djati, M. S. (2022). Potential of bioactive compound of *Cyperus rotundus* L. rhizome extract as inhibitor of PD-L1/PD-1 interaction: an *insilico* study. *Agriculture and Natural Resources*, 56(6), 751–760.
- [59] Jha, V., Devkar, S., Gharat, K., et al. (2022). Screening of phytochemicals as potential inhibitors of breast cancer using structure-based multitargeted molecular docking analysis. *Phytomedicine Plus*, 2, 100227.
- [60] Naveed, M., Ali, N., Aziz, T., Hanif, N., Fatima, M., Ali, I., Alharbi, M., Alasmari, A. F., & Albekairi, T. H. (2024). The natural breakthrough: phytochemicals as potent therapeutic agents against spinocerebellar ataxia type 3. *Scientific Reports*, 14(1), 1529.
- [61] Herowati, R., & Widodo, G. P. (2014). Molecular docking studies of chemical constituents of *Tinospora cordifolia* on glycogen phosphorylase. *Procedia Chemistry*, 13, 63–68.
- [62] Rathod, S., Shinde, K., Porlekar, J., Choudhari, P., Dhavale, R., Mahuli, D., Tamboli, Y., Bhatia, M., Haval, K. P., Al-Sehemi, A. G., & Pannipara, M. (2022). Computational exploration of anti-cancer potential of flavonoids against cyclin-dependent kinase 8: An *in silico* molecular docking and dynamic approach. *ACS Omega*, 8(1), 391–409.
- [63] Balaji NV, HariBabu B, Rao VU, Subbaraju GV, Nagasree KP, Kumar MMK. Synthesis, Screening and Docking Analysis of Hispolon Pyrazoles and Isoxazoles as Potential Antitubercular Agents. *Curr Top Med Chem*. 2019; 19(9):662-682.
- [64] BIOVIA, D. S. (2017). *Discovery Studio Visualizer* (p. 936). San Diego, CA: Dassault Systèmes.
- [65] Pandhi, S., & Poonia, A. (2019). Phytochemical screening of jamun seeds using different extraction methods. *The Pharma Innovation Journal*, 8, 226–231.
- [66] Kadry, H., Noorani, B., & Cucullo, L. (2020). A blood–brain barrier overview on structure, function, impairment, and biomarkers of integrity. *Fluids and Barriers of the CNS*, 17, 1–24.
- [67] Alajangi, H. K., Kaur, M., Sharma, A., Rana, S., Thakur, S., Chatterjee, M., Singla, N., Jaiswal, P. K., Singh, G., & Barnwal, R. P. (2022). Blood–brain barrier: Emerging trends on transport models and new-age strategies for therapeutic intervention against neurological disorders. *Molecular Brain*, 15, 1–28.
- [68] Karthika, C., Sureshkumar, R., Zehravi, M., Akter, R., Ali, F., Ramproshad, S., Mondal, B., Tagde, P., Ahmed, Z., & Khan, F. S. (2022). Multidrug resistance of cancer cells and the vital role of P-glycoprotein. *Life*, 12, 897.
- [69] Rachmale, M., Rajput, N., Jadav, T., Sahu, A. K., Tekade, R. K., & Sengupta, P. (2022). Implication of metabolomics and transporter modulation-based strategies to minimize multidrug resistance and enhance site-specific bioavailability: A needful consideration toward modern anticancer drug discovery. *Drug Metabolism Reviews*, 54, 101–119.
- [70] Attia, M. S., Elsebay, M. T., Yahya, G., Chopra, H., Marzouk, M., Yehya, A., & Abdelkhalek, A. S. (2023). Pharmaceutical polymers and P-glycoprotein: Current trends and possible outcomes in drug delivery. *Materials Today Communications*, 10, 105318.
- [71] Chatterjee, S., Jain, S., Jangid, R., & Sharma, M. K. (2022). Cytochrome P450 and P-gp mediated herb–drug interactions of some common Indian herbs. *Studies in Natural Products Chemistry*, 72, 225–258.
- [72] He, R., Dai, Z., Finel, M., Zhang, F., Tu, D., Yang, L., & Ge, G. (2023). Fluorescence-based high-throughput assays for investigating cytochrome P450 enzyme-mediated drug–drug interactions. *Drug Metabolism and Disposition*, 51, 1254–1272.
- [73] Xing, Y., Yu, Q., Zhou, L., Cai, W., Zhang, Y., Bi, Y., Zhang, Y., Fu, Z., & Han, L. (2023). Cytochrome P450-mediated herb-

drug interaction of *Polygonum multiflorum* Thunb. based on pharmacokinetic studies and in vitro inhibition assays. *Phytomedicine*, 112, 154710.

- [74] Azman, M., Sabri, A. H., Anjani, Q. K., Mustaffa, M. F., & Hamid, K. A. (2022). Intestinal absorption study: Challenges and absorption enhancement strategies in improving oral drug delivery. *Pharmaceuticals*, 15, 975.
- [75] Kumari, S., Saini, R., & Mishra, A. (2023). Phytochemical profiling and evaluation of the antidiabetic potential of *Ichnocarpus frutescens* (Krishna Sariva): Kinetic study, molecular modelling, and free energy approach. *Journal of Biomolecular Structure and Dynamics*.
- [76] Singh, I., Das, R., & Kumar, A. (2023). Network pharmacology-based anti-colorectal cancer activity of piperlonguminine in the ethanolic root extract of *Piper longum* L. *Medical Oncology*, 40, 320.
- [77] Saganuwan, S. A. (2017). Toxicity studies of drugs and chemicals in animals: An overview. *Bulgarian Journal of Veterinary Medicine*, 20(4), 291–318.